
DistPred: A Distribution-Free Probabilistic Inference Method for Regression and Forecasting

Daojun Liang

School of Information Science
and Engineering, Shandong University
liangdaojun@mail.sdu.edu.cn

Haixia Zhang

School of Control Science
and Engineering, Shandong University
haixia.zhang@sdu.edu.cn

Dongfeng Yuan

School of Qilu Transportation,
Shandong University
dfyuan@sdu.edu.cn

Abstract

Traditional regression and prediction tasks often only provide deterministic point estimates. To estimate the distribution or uncertainty of the response variable, traditional methods either assume that the posterior distribution of samples follows a Gaussian process or require thousands of forward passes for sample generation. We propose a novel approach called DistPred for regression and forecasting tasks, which overcomes the limitations of existing methods while remaining simple and powerful. Specifically, we transform proper scoring rules that measure the discrepancy between the predicted distribution and the target distribution into a differentiable discrete form and use it as a loss function to train the model end-to-end. This allows the model to sample numerous samples in a single forward pass to estimate the potential distribution of the response variable. We have compared our method with several existing approaches on multiple datasets and achieved state-of-the-art performance. Additionally, our method significantly improves computational efficiency. For example, compared to state-of-the-art models, DistPred has a 180x faster inference speed. Experimental results can be reproduced through this Repository.

1 Introduction

Traditional deterministic point estimates are no longer sufficient to meet the needs of AI safety and uncertainty quantification. For example, we may want to obtain confidence intervals for predicted points to make important decisions, such as deciding whether to travel based on weather forecasts or how to invest based on stock predictions. Moreover, this is particularly important in high-security AI application areas such as autonomous driving, risk estimation, and decision-making.

In this paper, we consider the underlying distribution behind predicting the response variable because it reflects the confidence intervals at all levels. For example, based on this distribution, we can calculate confidence intervals, coverage rate, and uncertainty quantification at any level, as shown in Fig. 1. Currently, predicting the distribution of the response variable poses a challenge because at a specific moment, the response variable can only take on a single deterministic value. This point can be viewed as a ‘*representative*’ sample from its underlying distribution, but it fails to represent the overall state of the underlying distribution.

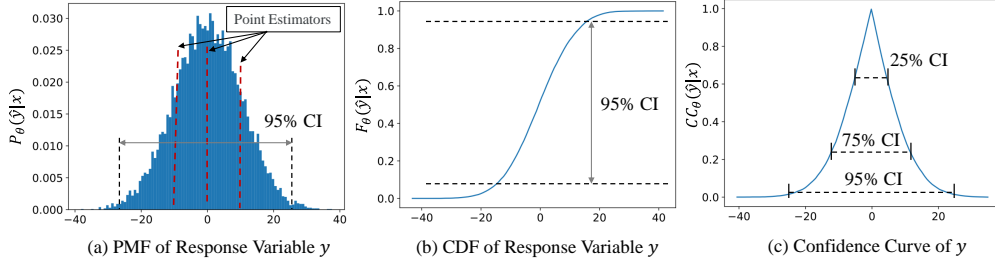


Figure 1: DistPred can provide K predicted values \hat{y} of the response variable y given the predictor variable x in a single forward process, denoted as $\mathbb{E}(\hat{Y}|x)$, where \hat{Y} represents a maximum likelihood sample of y . Based on this sampling, the probability mass function (PMF) $P_{\theta}(\hat{y}|x)$, cumulative distribution function (CDF) $F_{\theta}(\hat{y}|x)$, and confidence curve $CC_{\theta}(\hat{y}|x)$ for the response variable y can be computed, thereby yielding comprehensive statistical insights into y . For instance, this includes confidence intervals (CI) at any desired level, as well as p-values.

Currently, several methods are employed to predict the underlying distribution of the response variable in regression and forecasting tasks. The most straightforward approach is to assume that the response variable follows a prior distribution and represents a specific statistic from that distribution. Specifically, several methods (Bishop, 1994; Greene, 2003; Salinas et al., 2020; He et al., 2020) transform distribution prediction and uncertainty quantification into predicting statistical variables such as mean and variance by assuming that the response variable follows a known continuous distribution. For instance, mixture density networks (Bishop, 1994) superimpose a specific distribution, typically Gaussian, weighted by designated parameters to fit the prior distribution. Heteroscedasticity regression (Greene, 2003) quantifies uncertainty by modeling the variability of residuals as a function of independent variables. These methods only predict statistical variables, which reduces the inference cost, but strong assumptions often fail to capture the true data distribution, resulting in inferior performance.

Conformal prediction offers an alternative approach for distribution prediction (Vovk et al., 2017, 2018; Romano et al., 2019; Xu and Xie, 2021, 2023). The authors defined the random prediction system in (Vovk et al., 2017, 2018) and proposed a nonparametric prediction distribution method based on conformal assumptions. The authors integrated conformal prediction with quantile regression in (Romano et al., 2019; Xu and Xie, 2021, 2023) to construct prediction intervals for the response variable by training multiple bootstrap estimators. However, the application of conformal prediction to distribution prediction can be constrained by its reliance on the exchangeability assumption of residuals and the challenges in managing temporal dependencies (autocorrelation), potentially resulting in less reliable prediction intervals in non-i.i.d. data settings.

Uncertainty quantification is a method that indirectly reflects the potential distribution of the response variable, which can be classified into two primary categories: epistemic uncertainty and aleatoric uncertainty (Der Kiureghian and Ditlevsen (2009)). Epistemic uncertainty refers to the uncertainty within the model itself. In contrast, aleatoric uncertainty pertains to the inherent randomness in the observations. Quantitative analysis involves generating numerous samples (e.g., using MCMC) by perturbing the explanatory variables or models, thereby approximating the underlying distribution. For instance, Bayesian neural networks (BNNs) (Blundell et al., 2015; Immer et al., 2021; Daxberger et al., 2021) simulate this uncertainty by assuming that their parameters follow a predefined distribution, thereby capturing the model’s uncertainty given the data. Similarly, ensemble-based methods have been proposed to combine multiple deep models with random outputs to capture prediction uncertainty. MC Dropout (Gal and Ghahramani, 2016) shows that enabling dropout during each testing process yields results akin to model ensembling. Additionally, models based on GANs and diffusion have been introduced for conditional density estimation and prediction uncertainty quantification (Zhou et al., 2021b; Liu et al., 2021; Han et al., 2022). These models utilize noise during the generation or diffusion process to obtain different predicted values for estimating the uncertainty of the response variable.

The common characteristic of these methods mentioned above is the requirement of K forward passes to sample K representative samples. For example, Bayesian framework-based methods require K learnable parameter samples to be inferred in order to obtain K representative samples; ensemble

methods require K models to jointly infer; MC Dropout requires K forward passes with random dropout activations; generative models require K forward or diffusion processes. However, the excessive forward passes result in significant computational overhead and slow speed, a drawback that becomes increasingly apparent for AI applications with high real-time requirements.

To address this issue, we propose a novel method called DistPred, which is a distribution-free probabilistic inference method for regression and forecasting tasks. DistPred is a simple and powerful method that can estimate the distribution of the response variable in a single forward pass. Specifically, we contemplate employing all predictive quantiles to specify the potential cumulative density function (CDF) of the predictor variable, and we show that the full quantiles’ prediction can be translated into calculating the minimum expected score of the response variable and the predictive ensemble variables. Based on this, we transform proper scoring rules that measure the discrepancy between the predicted distribution and the target distribution into a differentiable discrete form and use it as a loss function to train the model end-to-end. This allows the model to sample numerous samples in a single forward pass to estimate the potential distribution of the response variable. DistPred is orthogonal to other methods, enabling its combination with alternative approaches to enhance estimation performance. Further, we show that DistPred can provide comprehensive statistical insights into the response variable, including confidence intervals at any desired level, p-values, and other statistical information, as shown in Fig. 1. Experimental results show that DistPred outperforms existing methods in terms of both accuracy and computational efficiency. Specifically, DistPred has a 180x faster inference speed than state-of-the-art models.



Figure 2: The workflow of DistPred. An ensemble of predictive variables \hat{Y} is inferred in a forward pass and $S(\mathbb{E}(\hat{Y}|x), y)$ is utilized to train the learner end-to-end.

2 Method

Assume that the dataset $D = \{x_i, y_i\}_{i=1}^N$ consists of N sample-label pairs. The subscript i will be omitted if it does not cause ambiguity in the context. Our objective is to utilize a machine learning model M with parameters θ to predict the underlying distribution $P(y|x)$ from D , aiming to acquire comprehensive statistical insights such as obtaining confidence intervals (CI) and quantifying uncertainty at any desired level.

Direct prediction of distribution $P_\theta(\hat{y}|x)$ is not feasible because:

1. Without distributional assumptions, we cannot give a valid representation of the PDF or CDF for the response variable.
2. We have only a deterministic target point, without access to its distribution information, which limits our ability to guide the model’s learning process.

To address the aforementioned issues, we contemplate employing full predictive quantiles $\hat{q}_1, \hat{q}_2, \dots, \hat{q}_K$ at levels $\alpha_1, \alpha_2, \dots, \alpha_K$, ($K \rightarrow \infty$), to specify the potential CDF $F_\theta(\hat{y})$ of the response variable \hat{y} . This is because if we know the cumulative distribution function of a random variable, we can find any quantile by

$$q_\alpha = \inf\{y \in \mathbb{R} : F(y) \geq \alpha\}. \quad (1)$$

Conversely, if we have a complete set of quantiles, we can approximate or reconstruct the cumulative distribution function of the random variable

$$F(y) = \sup\{\alpha \in [0, 1] : q_\alpha \leq y\}. \quad (2)$$

Full quantiles provide discrete ‘snapshots’ of the distribution, while the CDF is a continuous, smooth version of these snapshots, offering a complete description of the cumulative probability from the minimum to the maximum value.

2.1 Property of Full Quantiles

We contemplate probabilistic predictions pertaining to a continuous quantity, manifested as full predictive quantiles $\hat{q}_1, \dots, \hat{q}_K, (K \rightarrow \infty)$. For $P \in \mathcal{P}$, let $\hat{q}_1, \dots, \hat{q}_K$ denote the true P -quantiles at levels $\alpha_1, \dots, \alpha_K \in (0, 1)$. Then, the expected score $S(q_1, \dots, q_K; P)$ can be defined as

$$S(\hat{q}_1, \dots, \hat{q}_K; P) = \int S(\hat{q}_1, \dots, \hat{q}_K; y) dP(y). \quad (3)$$

The function S in Eq. 3 satisfies the scoring rule, which offers a concise measure for assessing probabilistic forecasts by assigning numerical scores according to the forecast distribution and predicted outcomes (Gneiting and Raftery, 2007; Jordan et al., 2017). Specifically, let Ω denote the set of possible values of the quantity of interest, and let \mathcal{P} denote a convex class of probability distributions on Ω , the scoring rule is a function

$$S: \Omega \times \mathcal{P} \rightarrow \mathbb{R} \cup \{\infty\} \quad (4)$$

that assigns numerical values to pairs of forecasts $P \in \mathcal{P}$ and observations $y \in \Omega$. We identify probabilistic forecasts P with the associated CDF F or PDF f , and consider scoring rules to be negatively oriented, where a lower score signifies a more accurate forecast. A proper scoring rule is optimized when the forecast aligns with the true distribution of the observation, i.e., if

$$E_{y \sim Q}[S(Q, y)] \leq E_{y \sim Q}[S(P, y)] \quad (5)$$

for all $P, Q \in \mathcal{P}$. A scoring rule is termed strictly proper when equality is achieved only when $P = Q$. Proper scoring rules are essential for comparative evaluation, especially in ranking forecasts.

Based on this definition, we can get the scoring rule S is proper when $S(q_1, \dots, q_K; P) \geq S(\hat{q}_1, \dots, \hat{q}_K; P)$. Further, assuming that s_k is a non-decreasing probability measure of \mathcal{P} , then the scoring rule

$$S(\hat{q}_1, \dots, \hat{q}_K; P) = \sum_{k=1}^K (\alpha_k s_k(\hat{q}_k) + (s_k(y) - s_k(\hat{q}_k)) \mathbb{I}\{y \leq \hat{q}_k\}) \quad (6)$$

is proper for predicting the quantiles at levels $\alpha_1, \dots, \alpha_K$ when $K \rightarrow \infty$ (Gneiting and Raftery, 2007; Schervish et al., 2012). $\mathbb{I}\{y \leq \hat{q}_k\}$ denotes the indicator function which is 1 if $y \leq \hat{q}_k$ and 0 otherwise.

2.2 Predicting CDF by Full Quantiles

Eq. 6 shows that full predictive quantiles are proper. Consequently, we can formulate scoring rules for the predictive distribution based on the scoring rules for the quantiles. Specifically, let S_α denote a proper scoring rule for the quantile at level α , then the scoring rule

$$S(F, y) = \int_0^1 S_\alpha(F^{-1}(\alpha); y) d\alpha = \int_{-\infty}^{\infty} S(F(\hat{y}), \mathbb{I}\{y \leq \hat{y}\}) d\hat{y} \quad (7)$$

is proper. Here, we establish a relationship between the full quantiles of the response variable and its CDF. However, the CDF here is in continuous form and cannot be directly observed. Therefore, we need to convert it into a discrete form, as the number of quantiles K is always finite in practice. It is worth noting that Eq. 7 corresponds to the continuous ranked probability score (CRPS) in which S is the quadratic or Brier score, defined as

$$C(F, y) = \int_{-\infty}^{\infty} (F(\hat{y}) - \mathbb{I}\{y \leq \hat{y}\})^2 d\hat{y}. \quad (8)$$

When the first moment of F is finite, the CRPS can be written as

$$C(F, y) = \mathbb{E}_F[|\hat{Y} - y|] - \frac{1}{2} \mathbb{E}_F[|\hat{Y} - \hat{Y}'|], \quad (9)$$

where \hat{Y} and \hat{Y}' denote independent predictive ensemble variables with distribution F .

Eq. 9 incentivizes forecasters to accurately report their perception of the true distribution in this scenario. Therefore, it provides attractive measures and utility functions that can be tailored to a

regression or forecast problem. To estimate θ , we need to measure the goodness-of-fit by the mean score

$$C_N(\theta) = \frac{1}{N} \sum_{i=1}^N C(F_\theta(\hat{y}_i), y_i). \quad (10)$$

Let θ^* denote the true parameter value, then asymptotic arguments indicate that $\operatorname{argmin}_\theta C_N(\theta) \rightarrow \theta^*$ as $N \rightarrow \infty$. As shown in Fig. 2, the workflow suggests a general approach to transforming proper scoring rules into loss functions for training models, which implicitly minimizes the discrepancy between predictive and true distributions.

2.3 End-to-End Ensemble Inference

Based on the analysis provided above, it is evident that predicting the full quantiles is equivalent to minimizing Eq. 9 w.r.t $\mathbb{E}(\hat{Y}|y)$. Hence, as illustrated in the architecture depicted in Fig. 3, we can develop a model M with parameters θ that infers an ensemble of predictive variables $\hat{Y} = \{\hat{y}_1, \dots, \hat{y}_K\}$ in a forward pass and utilize Eq. 10 to train it end-to-end. This allows the model to sample numerous samples in a single forward pass to estimate the empirical CDF \hat{F} by the predictive ensemble variables

$$C(\hat{F}, y) = \frac{1}{K} \sum_{k=1}^K |\hat{y}_k - y| - \frac{1}{2K^2} \sum_{k=1}^K \sum_{j=1}^K |\hat{y}_k - \hat{y}_j|. \quad (11)$$

It's worth noting that Eq. 11 is a differentiable discrete form w.r.t \hat{Y} and \hat{Y}' that strictly satisfies proper scoring rules. However, implementations of Eq. 11 exhibit inefficiency due to their storage complexity of $\mathcal{O}(K^2)$. This can be enhanced by using algebraically equivalent representations based on the generalized quantile function (Laio and Tamea, 2007) and the sorted predictive ensemble variables \vec{y}_k ,

$$C(\hat{F}, y) = \frac{1}{2K^2} \sum_{k=1}^K (\vec{y}_k - y)(k\mathbb{I}\{y \leq \vec{y}_k\} - k + \frac{1}{2}). \quad (12)$$

Since a sorting operation is involved, the storage complexity of Eq. 12 is $\mathcal{O}(K \log K)$. However, since Eq. 12 renders the objective $C(\hat{F}, y)$ non-differentiable, we employ probability-weighted moment estimation form to approximate it, as

$$C(\hat{F}, y) = \frac{1}{K} \sum_{k=1}^K |\hat{y}_k - y| + \frac{1}{K} \sum_{k=1}^K \hat{y}_k - \frac{2}{K(K-1)} \sum_{k=1}^K \hat{y}_k(k-1). \quad (13)$$

Actually, according to the definition of L-Moments, we can prove that the last term of Eq. 11 can be decomposed into the 1-th and 0-st order L-moments of Eq. 13, i.e., Eq. 13 is an unbiased estimate of Eq. 11 when it has a finite first L-moment. To conserve memory, we suggest utilizing Eq. 13, which has a storage complexity of $\mathcal{O}(K)$, as the loss function, since predicting ensemble variables in long-term forecasting tasks may lead to out-of-memory issues on GPUs.

2.4 Incorporate Alternative Methodologies

DistPred is orthogonal to other methods, enabling its combination with alternative approaches to enhance estimation performance. Here, with a focus on computational efficiency and memory conservation, we opt to integrate MC Dropout with DistPred, thereby denoting the amalgamation as **DistPred+MCD**. In our experiments, we observed that using DistPred+MCD can further enhance uncertainty quantification performance, albeit with a marginal increase in computational effort.

3 Experiments

In this paper, our focus centers on regression (proposed by Hernández-Lobato and Adams (2015)) and prediction (proposed by Zhou et al. (2021a)) tasks, where we validate the application of the proposed DistPred method to these specific endeavors.

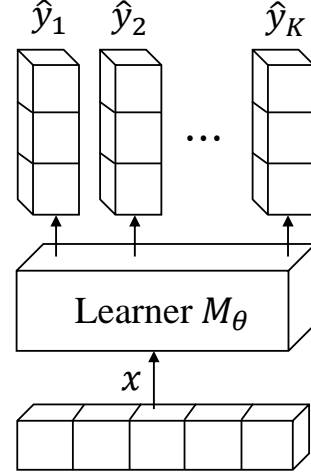


Figure 3: DistPred’s architecture. A model M with parameters θ takes one input variable x and outputs an ensemble of K response variable $\hat{y}_1, \dots, \hat{y}_K$.

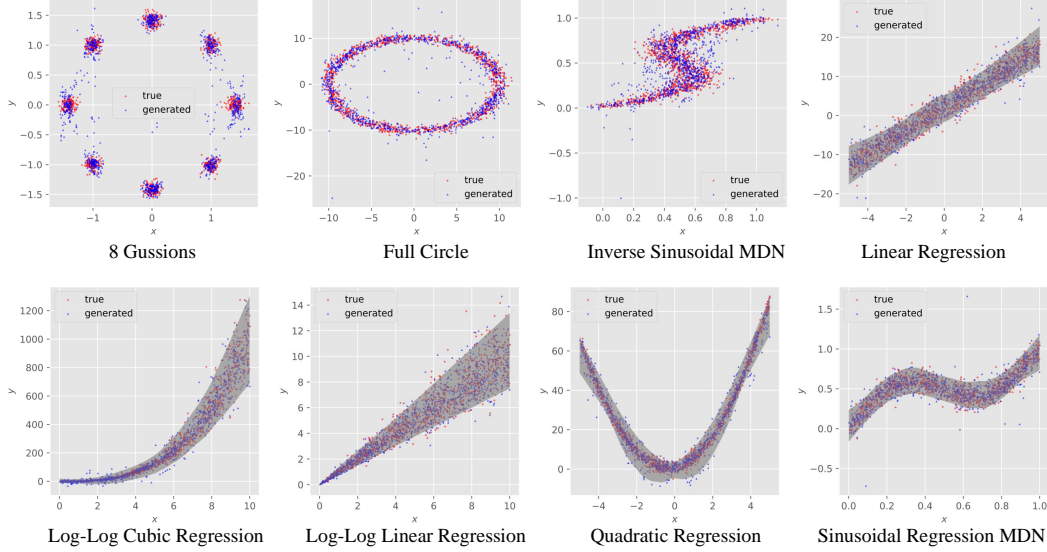


Figure 4: Scatter plot of DistPred’s regression results on 8 toy examples.

3.1 PICP and QICE Metrics

The metric utilized in BNNs to assess uncertainty estimates, namely the negative log-likelihood (NLL), is computed based on Gaussian prior. This assumption implies that they consider both the conditional distribution $p(y|x = x')$ for all x' are Gaussian. However, this assumption is very difficult to verify for real-world datasets. We follow (Han et al., 2022) and use the following two metrics, both of which are designed to empirically evaluate the degree of similarity between learned and true conditional distributions:

- **PICP** (Prediction Interval Coverage Probability) (Yao et al., 2019) is a metric that measures the proportion of true labels that fall within the prediction interval.
- **QICE** (Quantile Interval Calibration Error) (Han et al., 2022) is a metric that measures the average difference between the predicted and true quantiles at a given level α .

The PICP is calculated as

$$PICP := \frac{1}{N} \sum_{n=1}^N \mathbb{I}\{\hat{y}_n \geq q_{\alpha/2}\} \cdot \mathbb{I}\{\hat{y}_n \leq q_{1-\alpha/2}\}, \quad (14)$$

where $q_{\alpha/2}$ and $q_{1-\alpha/2}$ represent the low and high percentiles, respectively, that we have selected for the predicted \hat{y} outputs given the same x input. This metric evaluates the proportion of accurate observations that lie within the percentile range of the generated \hat{y} samples corresponding to each x input. Within this study, we opt for the 2.5th and 97.5th percentiles, signifying that an optimal PICP value for the model should ideally reach 95%.

However, a caveat of the PICP metric becomes apparent in the measurement of distribution differences. Drawing from this reasoning, Han et al. (2022) introduces a novel empirical metric called QICE. This metric can be perceived as an enhanced version of PICP, offering finer granularity and addressing the issue of uncovered quantile ranges. To calculate QICE, the initial step involves generating an adequate number of samples for each \hat{y} value. These samples are then divided into M bins of approximately equal sizes. Subsequently, the quantile values are determined at each boundary within these bins. The definition of QICE entails computing the mean absolute error (MAE) between the proportion of true data encompassed by each quantile interval and the optimal proportion, which is $1/M$ for all intervals:

$$QICE := \frac{1}{M} \sum_{m=1}^M \left| r_m - \frac{1}{M} \right|, \quad (15)$$

$$\text{where } r_m = \frac{1}{N} \sum_{n=1}^N \mathbb{I}\{\hat{y}_n \geq q_{\alpha/2}\} \cdot \mathbb{I}\{\hat{y}_n \leq q_{1-\alpha/2}\}.$$

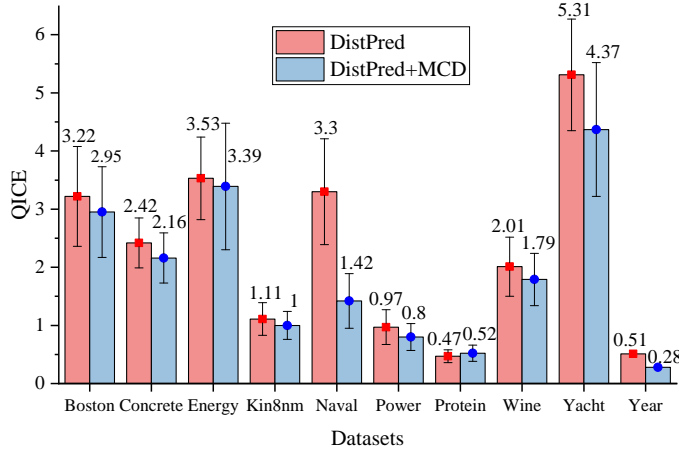


Figure 5: DistPred and DistPred+MCD on UCI datasets.

In this paper, we followed (Han et al., 2022) and set $M = 10$ for all experiments.

3.2 Toy Examples

To demonstrate the effectiveness of DistPred, we initially conducted experiments on 8 toy examples as done in (Han et al., 2022). These examples are specifically crafted with distinct statistical characteristics in their data generating functions: some have a uni-modal symmetric distribution for their error term (linear regression, quadratic regression, sinusoidal regression), while others exhibit heteroscedasticity (log-log linear regression, log-log cubic regression) or multi-modality (inverse sinusoidal regression, 8 Gaussians, full circle).

The research demonstrates that a trained DistPred model has the capability to produce samples that closely resemble the true response variable for novel covariates. Additionally, it can quantitatively match the true distribution based on certain summary statistics. The study visualizes scatter plots comparing real and generated data for all eight tasks in Fig. 4. In cases where the tasks involve unimodal conditional distributions, the interest region fills the region between the 2.5th and 97.5th percentiles of the generated \hat{y} values.

We note that within every task, the generated samples seamlessly integrate with the authentic test instances, indicating the potential of DistPred to reconstruct the inherent data generation process. This experiment visually demonstrates that DistPred effectively reconstructs the sample potential distribution of the target response variable. This indicates that the advantages of DistPred mentioned earlier can be fully harnessed in distribution prediction.

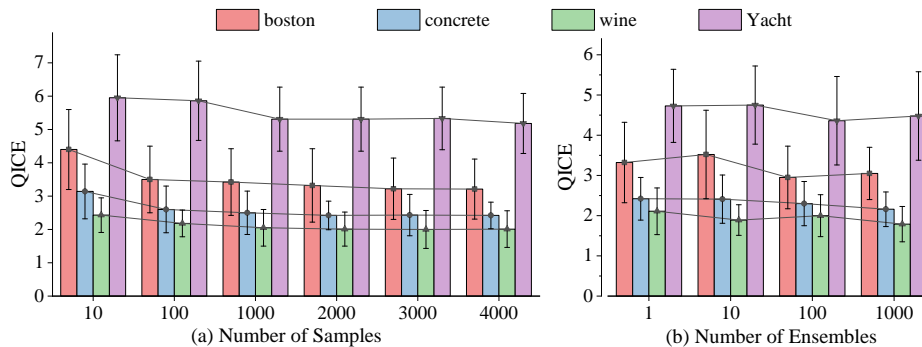


Figure 6: Ablation studies of the number of samples in DistPred (a) and the number of ensembles in DistPred+MCD (b).

Table 1: Comparison of model training and inference times (minutes) on UCI regression datasets when $K = 1000$.

Models	DistPred	DistPred+MCD	PBP	MC Dropout	CARD
Training	$0.035 \pm 6E-3$	$0.035 \pm 6E-3$	$0.04 \pm 8E-3$	0.031 ± 0.01	8.14 ± 0.05
Inference	$0.026 \pm 4E-3$	$0.027 \pm 5E-3$	5.23 ± 0.10	4.62 ± 0.06	8.31 ± 0.17

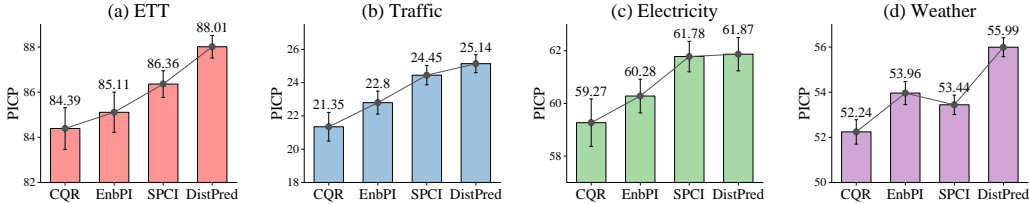


Figure 7: Comparison DistPred (ours) with conformal prediction methods. All results are averaged across all prediction lengths.

3.3 UCI Regression Tasks

For experiments conducted on real-world datasets, we utilize the same 10 UCI regression benchmark datasets (Asuncion and Newman, 2007) and follow the experimental protocol introduced by Hernández-Lobato and Adams (2015), which has also been followed by Gal and Ghahramani (2016) and Lakshminarayanan et al. (2017), as well as by Han et al. (2022). The dataset information can be found in Table 7 located in Appendix A.

We compare DistPred with other state-of-the-art methods, including PBP (Hernández-Lobato and Adams, 2015), MC Dropout (Gal and Ghahramani, 2016), DeepEnsemble (Lakshminarayanan et al., 2017), and another deep generative model that estimates a conditional distribution sampler, GCDS (Zhou et al., 2021b), as well as the diffusion model, CARD (Han et al., 2022). The multiple train-test splits are applied with a 90%/10% ratio, following the same methodology as Hernández-Lobato and Adams (2015) and Han et al. (2022) (20 folds for all datasets except 5 for Protein and 1 for Year). The reported metrics are presented as the mean and standard deviation across all splits. As pointed out by Han et al. (2022), we compare the QICE of different methods on various UCI datasets. Additional information regarding the experimental setup for these models is available in Appendix A.2. The experimental results, along with corresponding metrics, are presented in Table 2. The frequency with which each model achieves the best corresponding metric is reported in the penultimate row, while the frequency with which it achieves the top two positions is reported in the last row.

The results demonstrate that DistPred outperforms existing methods, often by a considerable margin. It is worth noting that these impressive results are achieved in a single forward pass of the DistPred method. Crucially, as shown in Fig. 5, the performance of uncertain quantization can be further enhanced by leveraging DistPred+MCD, a hybrid approach that combines DistPred and MC Dropout.

Table 2: QICE \downarrow (in %) of UCI regression tasks.

Dataset	PBP	MC Dropout	Deep Ensembles	GCDS	CARD	DistPred	DistPred-MCD
Boston	3.50 ± 0.88	3.82 ± 0.82	3.37 ± 0.00	11.73 ± 1.05	3.45 ± 0.83	3.22 ± 0.86	2.95 ± 0.78
Concrete	2.52 ± 0.60	4.17 ± 1.06	2.68 ± 0.64	10.49 ± 1.01	2.30 ± 0.66	2.42 ± 0.43	2.16 ± 0.43
Energy	6.54 ± 0.90	5.22 ± 1.02	3.62 ± 0.58	7.41 ± 2.19	4.91 ± 0.94	3.73 ± 0.71	3.39 ± 1.09
Kin8nm	1.31 ± 0.25	1.50 ± 0.32	1.17 ± 0.22	7.73 ± 0.80	0.92 ± 0.25	1.11 ± 0.28	1.00 ± 0.24
Naval	4.06 ± 1.25	12.50 ± 1.95	6.64 ± 0.60	5.76 ± 2.25	0.80 ± 0.21	3.30 ± 0.91	1.42 ± 0.47
Power	0.82 ± 0.19	1.32 ± 0.37	1.09 ± 0.26	1.77 ± 0.33	0.92 ± 0.21	0.97 ± 0.30	0.80 ± 0.23
Protein	1.69 ± 0.09	2.82 ± 0.41	2.17 ± 0.16	2.33 ± 0.18	0.71 ± 0.11	0.47 ± 0.11	0.52 ± 0.14
Wine	2.22 ± 0.64	2.79 ± 0.56	2.37 ± 0.63	3.13 ± 0.79	3.39 ± 0.69	2.01 ± 0.51	1.79 ± 0.45
Yacht	6.93 ± 1.74	10.33 ± 1.34	7.22 ± 1.41	5.01 ± 1.02	8.03 ± 1.17	5.31 ± 0.96	4.37 ± 1.15
Year	$2.96 \pm NA$	$2.43 \pm NA$	$2.56 \pm NA$	$1.61 \pm NA$	$0.53 \pm NA$	$0.58 \pm NA$	$0.28 \pm NA$
# Top 1	0	0	0	0	2	1	7
# Top 2	2	0	2	1	6	9	10

Table 3: Multivariate time series forecasting results on six benchmark datasets.

Model	DistPred					iTransformer		PatchTST		SCINet		TimesNet		DLinear		FEDformer		Autoformer		Informer		
Input Length	96					96		336		168		96		336		96		96		96		
Output	CRPS	QICE	PICP	MSE	MAE	MSE	MAE	MSE	MAE	MSE	MAE	MSE	MAE	MSE	MAE	MSE	MAE	MSE	MAE	MSE	MAE	
ETT	96	0.248	9.53	48.50	0.288	0.334	0.297	0.349	0.302	0.348	0.707	0.621	0.340	0.374	0.333	0.387	0.358	0.397	0.346	0.388	3.755	1.525
	336	0.277	9.22	51.06	0.348	0.371	0.380	0.400	0.388	0.400	0.860	0.689	0.402	0.414	0.477	0.476	0.429	0.439	0.456	0.452	5.602	1.931
	720	0.298	8.91	53.28	0.392	0.402	0.428	0.432	0.426	0.433	1.000	0.744	0.452	0.452	0.594	0.541	0.496	0.487	0.482	0.486	4.721	1.835
	720	0.322	8.23	57.11	0.437	0.436	0.427	0.445	0.431	0.446	1.249	0.838	0.462	0.468	0.831	0.657	0.463	0.474	0.515	0.511	3.647	1.625
	Avg	0.286	8.97	52.45	0.366	0.386	0.383	0.407	0.387	0.407	0.954	0.723	0.414	0.427	0.559	0.515	0.437	0.449	0.450	0.459	4.431	1.729
Traffic	96	0.193	12.75	34.85	0.391	0.251	0.395	0.268	0.544	0.359	0.788	0.499	0.593	0.321	0.650	0.396	0.587	0.366	0.613	0.388	0.719	0.391
	192	0.197	12.81	34.06	0.416	0.269	0.417	0.276	0.540	0.354	0.830	0.505	0.617	0.336	0.598	0.370	0.604	0.373	0.616	0.382	0.696	0.379
	336	0.202	12.90	34.03	0.427	0.275	0.433	0.283	0.551	0.358	0.558	0.508	0.629	0.336	0.605	0.373	0.621	0.383	0.622	0.337	0.777	0.420
	720	0.218	-	-	0.467	0.297	0.467	0.302	0.586	0.375	0.841	0.523	0.640	0.350	0.645	0.394	0.626	0.382	0.660	0.408	0.864	0.472
	Avg	0.203	-	-	0.425	0.273	0.428	0.282	0.555	0.362	0.804	0.509	0.620	0.336	0.625	0.383	0.610	0.376	0.628	0.379	0.764	0.416
Electricity	96	0.167	12.16	34.11	0.138	0.231	0.148	0.240	0.195	0.285	0.247	0.345	0.168	0.272	0.197	0.282	0.193	0.308	0.201	0.317	0.274	0.368
	192	0.178	11.62	38.85	0.155	0.246	0.162	0.253	0.199	0.289	0.257	0.355	0.184	0.289	0.196	0.285	0.201	0.315	0.222	0.334	0.296	0.386
	336	0.188	11.14	41.27	0.169	0.264	0.178	0.269	0.215	0.305	0.269	0.369	0.198	0.300	0.209	0.301	0.214	0.329	0.231	0.338	0.300	0.394
	720	0.209	10.79	42.83	0.207	0.298	0.225	0.317	0.256	0.337	0.299	0.390	0.220	0.320	0.245	0.333	0.246	0.355	0.254	0.361	0.373	0.439
	Avg	0.186	11.45	39.27	0.167	0.260	0.178	0.270	0.216	0.304	0.268	0.365	0.192	0.295	0.212	0.300	0.214	0.327	0.227	0.338	0.311	0.397
Weather	96	0.145	12.05	29.96	0.152	0.192	0.174	0.214	0.177	0.218	0.221	0.306	0.172	0.220	0.196	0.255	0.217	0.296	0.266	0.336	0.300	0.384
	192	0.185	10.607	39.85	0.210	0.247	0.221	0.254	0.225	0.259	0.261	0.340	0.219	0.261	0.237	0.296	0.276	0.336	0.307	0.367	0.598	0.544
	336	0.216	9.857	44.84	0.263	0.286	0.278	0.296	0.278	0.297	0.309	0.378	0.280	0.306	0.283	0.335	0.339	0.380	0.359	0.395	0.578	0.523
	720	0.263	9.31	47.83	0.362	0.349	0.358	0.349	0.354	0.348	0.377	0.427	0.365	0.359	0.345	0.381	0.403	0.428	0.419	0.428	1.059	0.741
	Avg	0.202	10.46	40.62	0.247	0.269	0.258	0.279	0.259	0.281	0.292	0.363	0.259	0.287	0.265	0.317	0.309	0.360	0.338	0.382	0.634	0.548
Solar	96	0.152	6.36	65.75	0.205	0.227	0.203	0.237	0.234	0.286	0.237	0.344	0.250	0.292	0.290	0.378	0.242	0.342	0.884	0.711	0.236	0.259
	192	0.165	8.39	53.34	0.236	0.251	0.233	0.261	0.267	0.310	0.280	0.380	0.296	0.318	0.320	0.398	0.285	0.380	0.834	0.692	0.217	0.269
	336	0.171	7.82	55.37	0.256	0.264	0.248	0.273	0.290	0.315	0.304	0.389	0.319	0.330	0.353	0.415	0.282	0.376	0.941	0.723	0.249	0.283
	720	0.187	8.79	55.15	0.273	0.278	0.249	0.275	0.289	0.317	0.308	0.388	0.338	0.337	0.356	0.413	0.357	0.427	0.882	0.717	0.241	0.317
	Avg	0.169	7.84	57.40	0.243	0.255	0.233	0.262	0.270	0.307	0.282	0.375	0.301	0.319	0.330	0.401	0.291	0.381	0.885	0.711	0.235	0.280
PEMS	12	0.120	9.01	52.99	0.064	0.166	0.071	0.174	0.099	0.216	0.066	0.172	0.085	0.192	0.122	0.243	0.126	0.251	0.272	0.385	0.126	0.233
	24	0.141	9.05	52.01	0.087	0.192	0.093	0.201	0.142	0.259	0.085	0.198	0.118	0.223	0.201	0.317	0.149	0.275	0.334	0.440	0.139	0.250
	36	0.170	8.41	57.39	0.124	0.233	0.125	0.236	0.211	0.319	0.127	0.238	0.155	0.260	0.333	0.425	0.227	0.348	1.032	0.782	0.186	0.289
	48	0.181	9.37	49.55	0.140	0.245	0.160	0.270	0.269	0.370	0.178	0.287	0.228	0.317	0.457	0.515	0.348	0.434	1.031	0.796	0.233	0.323
	Avg	0.153	8.96	52.99	0.104	0.209	0.113	0.221	0.180	0.291	0.114	0.224	0.147	0.248	0.278	0.375	0.213	0.327	0.667	0.601	0.171	0.274
# Top 1	-	-	-	22	28	5	1	0	1	1	0	0	0	0	0	0	0	0	0	0	2	0

The implementation of DistPred on UCI regression tasks follows a straightforward approach: We employ a basic multilayer perceptron (MLP) as the foundational framework, complemented by Eq. 13 serving as the loss function for end-to-end training. Due to the fact that DistPred necessitates solely a single forward inference, its inference speed is notably rapid. Table 1 presents a comparison of the training and inference speeds of mainstream models. It should be noted that, for a fair comparison, the implementations of various models are constructed on the same backbone and utilize the same equipment. It is evident that DistPred is approximately achieves at least 180x faster inference speed compared to state-of-the-art models. The inference speed of DistPred is slower than its training speed because it involves calculating distribution statistical metrics like QICE and PICP.

3.4 Ablation Study of The Number of Samples and Ensembles

We investigate the influence of the number of samples generated by DistPred, as well as the number of ensembles of DistPred+MCD, on their respective performances. In Fig. 6(a), we increase the number of samples of DistPred from 10 to 4000 to observe the changes in its QICE. In Fig. 6(b), we increase the number of ensembles of DistPred+MCD from 1 (DistPred) to 1000 to observe the changes in its QICE. It can be found that with an increase in the number of output samples and ensembles, the model’s performance shows a gradual improvement.

3.5 Time Series Distribution Forecasting

We extend time series forecasting (Zhou et al., 2021a; Wu et al., 2021; Zhou et al., 2022; Liu et al., 2023) from point estimation to the task of distribution prediction to infer about more statistical information about a certain moment.

Baselines: We employ recent 10 SOTA methods for comparisons, including iTransformer Liu et al. (2023), PatchTST Nie et al. (2022), SCINet Liu et al. (2022a), TimesNet Wu et al. (2022), DLinear Zeng et al. (2023), FEDformer Zhou et al. (2022), Autoformer Wu et al. (2021), Informer Zhou et al. (2021a), LogTrans Li et al. (2019) and Reformer Kitaev et al. (2020). DistPred employs the same network architecture as iTransformer. We use the same experimental setup as (Zhou et al., 2021a) and (Liu et al., 2022a) and follow the same experimental protocol as (Zhou et al., 2021a). Univariate results can be found in Appendix E.

Datasets and Setting: The detailed information pertaining to the datasets can be located in Appendix A. The models Liang et al. (2024) used in the experiments are evaluated over a wide range of prediction lengths to compare performance on different future horizons: 96, 192, 336, and 720. The experimental settings are the same for both multivariate and univariate tasks. We use the average of the MSE and MAE ($\frac{MSE+MAE}{2}$) to evaluate the overall performance of the model. It is noteworthy

Table 4: Stability experiments of loss function (Eq. 13).

	1%	25%	50%	75%	100%
Train Loss	0.21±0.04	0.174±0.03	0.165±0.01	0.162±0.01	0.16±0.007
Valid Loss	0.17±0.05	0.155±0.04	0.151±0.02	0.15±0.02	0.15±0.01

Table 5: KL-divergence, skewness, and kurtosis of the predictive response variable to the standard Gaussian on the ETTm2 datasets under input-96-predict-96 with $K = 100$.

Variates	1	2	3	4	5	6	7
KL-Div	0.11	0.1	inf	0.13	0.03	inf	0.05
Skewness	-0.42	0.41	-0.47	0.16	-0.03	-0.26	-0.72
Kurtosis	0.77	0.09	1.93	0.31	0.85	1.95	1.77

that DistPred provides an ensemble \hat{Y} of response variable. Consequently, we employ the mean value of \hat{Y} as the point estimate at that moment.

Main Results: The results for multivariate TS forecasting are outlined in Table 3, with the optimal results highlighted in **bold** and the second-best results emphasized with underlined. It can be found that, despite not utilizing MSE and MAE, DistPred achieves state-of-the-art performance across all datasets and prediction length configurations. iTransformer and PatchTST stand out as the latest models acknowledged for their exceptional average performance. Compared with them, the proposed DistPred demonstrates an average performance increase of **3.5%** and **16.5%**, respectively, achieving a substantial performance improvement. We provide metrics, e.g., CRPS, QICE, PICP, for comparison by the future research community. Note that for long time series, computing these metrics on the entire testset can be very time-consuming and may lead to out-of-memory issues. Therefore, we propose calculating these metrics for each batch and then averaging the results.

3.6 Comparison with Conformal Prediction

Since conformal prediction offers an alternative approach for distribution prediction, we compare DistPred with conformal prediction methods on the time series forecasting tasks, including CQR (Romano et al., 2019), EnbPI (Xu and Xie, 2021), SPCI (Xu and Xie, 2023). Since PICP is the primary metric used by these methods, we adhere to their convention in this work. As shown in Fig. 7, DistPred achieves better performance than conformal prediction methods on all datasets and prediction lengths, with an average PICP improvement of 4.5%. This further underscores the high competitiveness of DistPred.

3.7 Stability of The Loss Function

We included detailed discussions and experiments on the convergence and stability of the proposed method. As shown in Table 4, the experiments show that the training and valid loss converge smoothly across multiple runs, with no evidence of instability.

3.8 Visualization of The Predictive Distribution

We conducted thorough statistical analyses, including QQ-plots, histograms, and metrics like KL-divergence, skewness, and kurtosis, to validate the empirical distribution of the predictive response variable. KL-divergence, skewness, and kurtosis of the predictive response variable are shown in Table 5, and QQ-plots and histograms are shown in Fig. 8. These statistical analyses shows that the empirical distribution exhibits notable characteristics, such as skewness and heavy tails, etc., which are typical of many real-world datasets.

Furthermore, the predictive distribution of DistPred is visualized in Fig. 9. It can be observed that DistPred provides an ensemble of predictions (only the top 10 are presented in the left subplot). Given all predictive ensemble values, the model can estimate the distribution of the response variable. Consequently, we can calculate confidence intervals at different levels, as shown in the right subplot of Fig. 9.

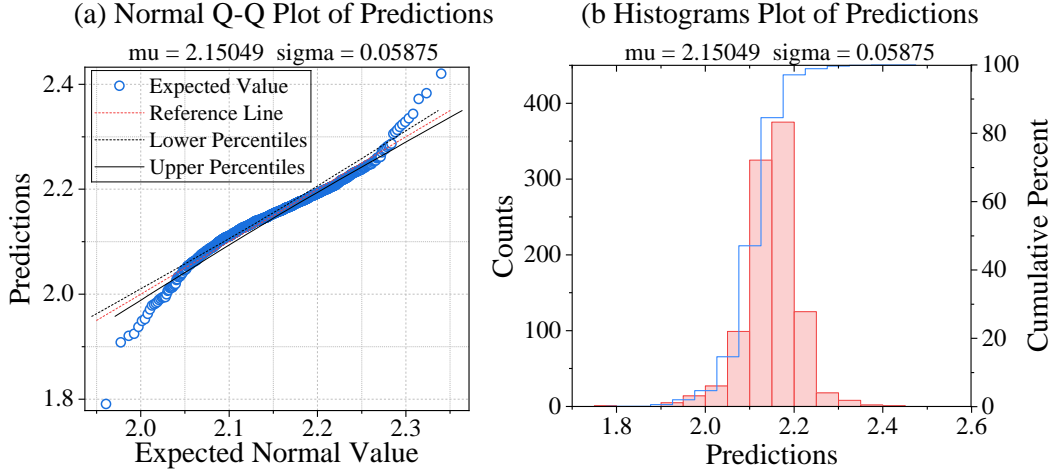


Figure 8: QQ-plots and histograms of response variable.

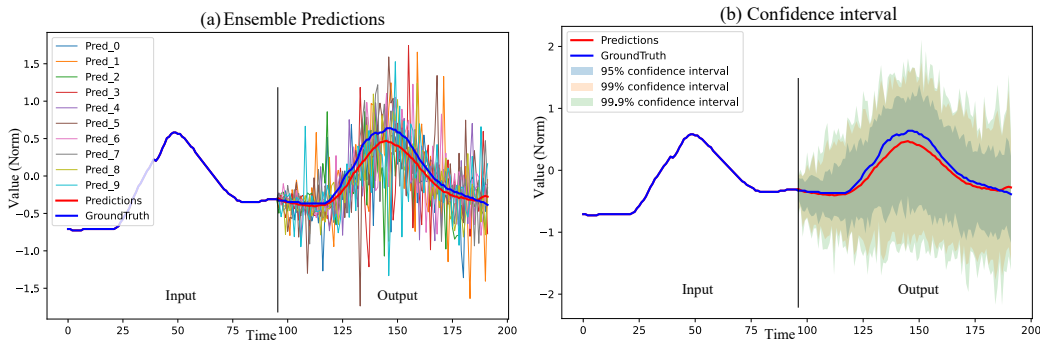


Figure 9: Visualization of the prediction results and the confidence intervals with setting input-96-predict-96 on the Etm2 dataset. (a) The left subplot shows the ensemble of predictions with $K = 100$. By utilizing subgraph (a), we can directly obtain the confidence intervals for subgraph (b), e.g, confidence intervals at 99%, 99.5% and 99.9% levels.

4 Related Work

In supervised learning contexts, the endeavor to characterize the conditional distribution $p(y|x)$ beyond merely the conditional mean $\mathbb{E}[y|x]$ via deep neural networks has been a focal point of existing research efforts. These endeavors primarily concentrate on quantifying uncertainty, with several approaches having been proposed.

In regression and forecasting tasks, predicting the underlying distribution of the response variable is pivotal. Traditional approaches (Bishop, 1994; Greene, 2003; Salinas et al., 2020; He et al., 2020) often rely on the assumption that the response variable conforms to a prior distribution, with the goal of estimating specific statistics derived from this distribution. Commonly, these methods transform the challenge of distribution prediction and uncertainty quantification into the prediction of statistical parameters such as the mean and variance, under the presumption of a known continuous distribution. For example, MDNs (Bishop, 1994) impose a predefined distribution—typically Gaussian—weighted by certain parameters to approximate the final distribution. Similarly, heteroscedastic regression (Greene, 2003) predicts uncertainty by modeling the variability of residuals as a function of independent variables. DeepAR (Salinas et al., 2020), another notable approach, assumes a Gaussian distribution for the response variable, thereby leveraging the GaussianNLLLoss (Nix and Weigend, 1994) to directly optimize its mean and variance. While these methods offer computational efficiency by simplifying predictions to statistical parameters, their reliance on strong distributional assumptions often limits their ability to capture the true underlying distribution, potentially leading to suboptimal performance.

Conformal prediction presents an alternative framework for distribution prediction, diverging from traditional parametric approaches. In their study, the authors in (Vovk et al., 2017, 2018) introduced a random prediction system and proposed a nonparametric prediction method grounded in conformal assumptions. By integrating conformal prediction with quantile regression in (Romano et al., 2019; Xu and Xie, 2021, 2023), they developed a method for constructing prediction intervals for the response variable. However, the practical application of conformal prediction is not without limitations. Its effectiveness is often constrained by the assumption of exchangeability of residuals, which may not hold in all contexts, particularly in the presence of temporal dependencies. This limitation can lead to less reliable prediction intervals when applied to non-independent and identically distributed (non-i.i.d.) data, thereby challenging its robustness in real-world scenarios where data often exhibit complex dependencies.

Uncertainty quantification is a method that indirectly reflects the potential distribution of the response variable. BNNs represent one such approach, aiming to capture such uncertainty by positing distributions over network parameters, thereby encapsulating the model’s plausibility given the available data (Blundell et al., 2015; Hernández-Lobato and Adams, 2015; Gal and Ghahramani, 2016; Kingma et al., 2015; Tomczak et al., 2021). Another avenue is represented by Kendall and Gal (2017), which not only addresses uncertainties in model parameters but also incorporates an additive noise term into the outputs to encompass uncertainties. In parallel, ensemble-based methodologies (Lakshminarayanan et al., 2017; Liu et al., 2022b) have emerged to address predictive uncertainty. These methods involve amalgamating multiple neural networks with stochastic outputs. Furthermore, the neural processes’ family (Garnelo et al., 2018b,a; Kim et al., 2019; Gordon et al., 2020) has introduced a suite of models tailored to capturing predictive uncertainty in a manner that extends beyond the distribution of available data, particularly tailored for few-shot learning.

The aforementioned models have predominantly operated under the assumption of a parametric form in $p(y|x)$, typically adopting a Gaussian distribution or a mixture of Gaussians. They optimize network parameters by minimizing the negative log-likelihood of a Gaussian objective function. In contrast, deep generative models are renowned for their capacity to model implicit distributions without relying on parametric distributional assumptions. However, only a sparse number of works have ventured into leveraging this capability to address regression tasks. GAN-based models, as introduced by Zhou et al. (2021b) and Liu et al. (2021), have emerged as one such endeavor, focusing on conditional density estimation and predictive uncertainty quantification. Additionally, Han et al. (2022) have proposed a diffusion-based model tailored for conditional density estimation. Nevertheless, it is imperative to note that these models entail protracted training processes and computationally demanding inference procedures.

5 Conclusion

In this paper, we propose a novel method named DistPred, which is a distribution-free probabilistic inference approach for regression and forecasting tasks. We transform proper scoring rules that measure the discrepancy between the predicted distribution and the target distribution into a differentiable discrete form and use it as a loss function to train the model end-to-end. This allows the model to sample numerous samples in a single forward pass to estimate the potential distribution of the response variable. Experimental results demonstrate that DistPred outperforms existing methods, often by a considerable margin. We also extend time series forecasting from point estimation to distribution prediction and achieve state-of-the-art performance on multivariate and univariate time series forecasting tasks. In the future, we plan to extend DistPred to other tasks, such as classification and reinforcement learning.

References

- Arthur Asuncion and David Newman. Uci machine learning repository, 2007.
- Christopher M Bishop. Mixture density networks. *Technical report*, 1994.
- Charles Blundell, Julien Cornebise, Koray Kavukcuoglu, and Daan Wierstra. Weight uncertainty in neural network. In Francis Bach and David Blei, editors, *Proceedings of the 32nd International Conference on Machine Learning*, volume 37 of *Proceedings of Machine Learning Research*, pages 1613–1622, Lille, France, 07–09 Jul 2015.
- Erik Daxberger, Agustinus Kristiadi, Alexander Immer, Runa Eschenhagen, Matthias Bauer, and Philipp Hennig. Laplace redux-effortless bayesian deep learning. *Advances in Neural Information Processing Systems*, 34:20089–20103, 2021.
- Armen Der Kiureghian and Ove Ditlevsen. Aleatory or epistemic? does it matter? *Structural safety*, 31(2):105–112, 2009.
- Yarin Gal and Zoubin Ghahramani. Dropout as a bayesian approximation: Representing model uncertainty in deep learning. In Maria Florina Balcan and Kilian Q. Weinberger, editors, *Proceedings of The 33rd International Conference on Machine Learning*, volume 48 of *Proceedings of Machine Learning Research*, pages 1050–1059, New York, New York, USA, 20–22 Jun 2016.
- Marta Garnelo, Dan Rosenbaum, Chris J. Maddison, Tiago Ramalho, David Saxton, Murray Shannahan, Yee Whye Teh, Danilo J. Rezende, and S. M. Ali Eslami. Conditional neural processes. In *Proceedings of the 35th International Conference on Machine Learning*, 2018a.
- Marta Garnelo, Jonathan Schwarz, Dan Rosenbaum, Fabio Viola, Danilo J. Rezende, S.M. Ali Eslami, and Yee Whye Teh. Neural processes. In *ICML 2018 workshop on Theoretical Foundations and Applications of Deep Generative Models*, 2018b.
- Tilmann Gneiting and Adrian E Raftery. Strictly proper scoring rules, prediction, and estimation. *Journal of the American statistical Association*, 102(477):359–378, 2007.
- Jonathan Gordon, Wessel P. Bruinsma, Andrew Y. K. Foong, James Requeima, Yann Dubois, and Richard E. Turner. Convolutional conditional neural processes. In *Proceedings of the 8th International Conference on Learning Representations*, 2020.
- WH Greene. Econometric analysis. *Prentice Hall google schola*, 3:116–125, 2003.
- Xizewen Han, Huangjie Zheng, and Mingyuan Zhou. Card: Classification and regression diffusion models. *Advances in Neural Information Processing Systems*, 35:18100–18115, 2022.
- Bobby He, Balaji Lakshminarayanan, and Yee Whye Teh. Bayesian deep ensembles via the neural tangent kernel. In H. Larochelle, M. Ranzato, R. Hadsell, M.F. Balcan, and H. Lin, editors, *Advances in Neural Information Processing Systems*, volume 33, pages 1010–1022. Curran Associates, Inc., 2020. URL https://proceedings.neurips.cc/paper_files/paper/2020/file/0b1ec366924b26fc98fa7b71a9c249cf-Paper.pdf.
- José Miguel Hernández-Lobato and Ryan Adams. Probabilistic backpropagation for scalable learning of bayesian neural networks. In *International conference on machine learning*, pages 1861–1869. PMLR, 2015.
- Alexander Immer, Maciej Korzepa, and Matthias Bauer. Improving predictions of bayesian neural nets via local linearization. In *International conference on artificial intelligence and statistics*, pages 703–711. PMLR, 2021.
- Alexander Jordan, Fabian Krüger, and Sebastian Lerch. Evaluating probabilistic forecasts with scoringrules. *arXiv preprint arXiv:1709.04743*, 2017.
- Alex Kendall and Yarin Gal. What uncertainties do we need in Bayesian deep learning for computer vision? In *Proceedings of the 31st Conference on Neural Information Processing Systems*, 2017.

- Hyunjik Kim, Andriy Mnih, Jonathan Schwarz, Marta Garnelo, Ali Eslami, Dan Rosenbaum, Oriol Vinyals, and Yee Whye Teh. Attentive neural processes. In *Proceedings of the 7th International Conference on Learning Representations*, 2019.
- Diederik P Kingma and Jimmy Ba. Adam: A method for stochastic optimization. In *International Conference on Learning Representations (ICLR)*, Santiago de Cuba, 2015.
- Durk P. Kingma, Tim Salimans, and Max Welling. Variational dropout and the local reparameterization trick. In *Proceedings of the 29th Conference on Neural Information Processing Systems*, 2015.
- Nikita Kitaev, Lukasz Kaiser, and Anselm Levskaya. Reformer: The efficient transformer. In *8th International Conference on Learning Representations (ICLR)*, Ababa, Ethiopia, 2020.
- Guokun Lai, Wei-Cheng Chang, Yiming Yang, and Hanxiao Liu. Modeling long- and short-term temporal patterns with deep neural networks. In *The 41st international ACM SIGIR conference on research & development in information retrieval (SIGIR)*, pages 95–104, Ann Arbor, MI, USA, 2018.
- Francesco Laio and Stefania Tamea. Verification tools for probabilistic forecasts of continuous hydrological variables. *Hydrology and Earth System Sciences*, 11(4):1267–1277, 2007.
- Balaji Lakshminarayanan, Alexander Pritzel, and Charles Blundell. Simple and scalable predictive uncertainty estimation using deep ensembles. *Advances in neural information processing systems*, 30, 2017.
- Shiyang Li, Xiaoyong Jin, Yao Xuan, Xiyou Zhou, Wenhui Chen, Yu-Xiang Wang, and Xifeng Yan. Enhancing the locality and breaking the memory bottleneck of transformer on time series forecasting. In *Advances in 33rd Neural Information Processing Systems (NeurIPS)*, volume 32, pages 5243–5253, Vancouver, Canada, 2019.
- Daojun Liang, Haixia Zhang, Dongfeng Yuan, Bingzheng Zhang, and Minggao Zhang. Minusformer: Improving time series forecasting by progressively learning residuals. *arXiv preprint arXiv:2402.02332*, 2024.
- Minhao Liu, Ailing Zeng, Muxi Chen, Zhijian Xu, Qiuxia Lai, Lingna Ma, and Qiang Xu. Scinet: Time series modeling and forecasting with sample convolution and interaction. In *Advances in Neural Information Processing Systems*, pages 5816–5828, 2022a.
- Shiao Liu, Xingyu Zhou, Yuling Jiao, and Jian Huang. Wasserstein generative learning of conditional distribution. *arXiv preprint arXiv:2112.10039*, 2021.
- Shiwei Liu, Tianlong Chen, Zahra Atashgahi, Xiaohan Chen, Ghada Sokar, Elena Mocanu, Mykola Pechenizkiy, Zhangyang Wang, and Decebal Constantin Mocanu. Deep ensembling with no overhead for either training or testing: The all-round blessings of dynamic sparsity. In *Proceedings of the 10th International Conference on Learning Representations*, 2022b.
- Yong Liu, Tengge Hu, Haoran Zhang, Haixu Wu, Shiyu Wang, Lintao Ma, and Mingsheng Long. itransformer: Inverted transformers are effective for time series forecasting. *arXiv preprint arXiv:2310.06625*, 2023.
- Yuqi Nie, Nam H Nguyen, Phanwadee Sinthong, and Jayant Kalagnanam. A time series is worth 64 words: Long-term forecasting with transformers. In *The Eleventh International Conference on Learning Representations*, 2022.
- D.A. Nix and A.S. Weigend. Estimating the mean and variance of the target probability distribution. In *Proceedings of 1994 IEEE International Conference on Neural Networks (ICNN'94)*, volume 1, pages 55–60 vol.1, 1994. doi: 10.1109/ICNN.1994.374138.
- Yaniv Romano, Evan Patterson, and Emmanuel Candes. Conformalized quantile regression. *Advances in neural information processing systems*, 32, 2019.
- David Salinas, Valentin Flunkert, Jan Gasthaus, and Tim Januschowski. Deepar: Probabilistic forecasting with autoregressive recurrent networks. *International journal of forecasting*, 36(3): 1181–1191, 2020.

- Mark J Schervish, Joseph B Kadane, and Teddy Seidenfeld. Characterization of proper and strictly proper scoring rules for quantiles. *Preprint, Carnegie Mellon University, March*, 18, 2012.
- Marcin B. Tomczak, Siddharth Swaroop, Andrew Y. K. Foong, and Richard E. Turner. Collapsed variational bounds for Bayesian neural networks. In *Proceedings of the 35th Conference on Neural Information Processing Systems*, 2021.
- Vladimir Vovk, Jieli Shen, Valery Manokhin, and Min-ge Xie. Nonparametric predictive distributions based on conformal prediction. In *Conformal and probabilistic prediction and applications*, pages 82–102. PMLR, 2017.
- Vladimir Vovk, Ilia Nouretdinov, Valery Manokhin, and Alexander Gammerman. Cross-conformal predictive distributions. In *conformal and probabilistic prediction and applications*, pages 37–51. PMLR, 2018.
- Haixu Wu, Jiehui Xu, Jianmin Wang, and Mingsheng Long. Autoformer: Decomposition transformers with auto-correlation for long-term series forecasting. In *Advances in Neural Information Processing Systems (NeurIPS)*, volume 34, pages 22419–22430, Virtual Conference, 2021.
- Haixu Wu, Tengge Hu, Yong Liu, Hang Zhou, Jianmin Wang, and Mingsheng Long. Timesnet: Temporal 2d-variation modeling for general time series analysis. In *The Eleventh International Conference on Learning Representations*, 2022.
- Chen Xu and Yao Xie. Conformal prediction interval for dynamic time-series. In *International Conference on Machine Learning*, pages 11559–11569. PMLR, 2021.
- Chen Xu and Yao Xie. Sequential predictive conformal inference for time series. In *International Conference on Machine Learning*, pages 38707–38727. PMLR, 2023.
- Jiayu Yao, Weiwei Pan, Soumya Ghosh, and Finale Doshi-Velez. Quality of uncertainty quantification for bayesian neural network inference. *arXiv preprint arXiv:1906.09686*, 2019.
- Ailing Zeng, Muxi Chen, Lei Zhang, and Qiang Xu. Are transformers effective for time series forecasting? In *Proceedings of the AAAI conference on artificial intelligence*, volume 37, pages 11121–11128, 2023.
- Haoyi Zhou, Shanghang Zhang, Jieqi Peng, Shuai Zhang, Jianxin Li, Hui Xiong, and Wancai Zhang. Informer: Beyond efficient transformer for long sequence time-series forecasting. In *Proceedings of the 35th AAAI Conference on Artificial Intelligence (AAAI)*, volume 35, pages 11106–11115, Virtual Conference, 2021a.
- Tian Zhou, Ziqing Ma, Qingsong Wen, Xue Wang, Liang Sun, and Rong Jin. FEDformer: Frequency enhanced decomposed transformer for long-term series forecasting. In *Proceedings of the 39th International Conference on Machine Learning (ICML)*, volume 162, pages 27268–27286, Baltimore, Maryland, 2022.
- Xingyu Zhou, Yuling Jiao, Jin Liu, and Jian Huang. A deep generative approach to conditional sampling. *Journal of the American Statistical Association*, pages 1–28, 2021b.

Table 6: Details of the seven TS datasets.

Dataset	length	features	frequency
ETTh1	17,420	7	1h
ETTh2	17,420	7	1h
ETTh1	69,680	7	15m
ETTh2	69,680	7	15m
Electricity	26,304	321	1h
Exchange	7,588	8	1d
Traffic	17,544	862	1h
Weather	52,696	21	10m
Solar	52,560	137	10m
PEMS	26,208	358	5m
Illness	966	7	7d

Table 7: Dataset size (N observations, P features) of UCI regression tasks.

Dataset	Boston	Concrete	Energy	Kin8nm	Naval	Power	Protein	Wine	Yacht	Year
(N, P)	(506, 13)	(1030, 8)	(768, 8)	(8192, 8)	(11, 934, 16)	(9568, 4)	(45, 730, 9)	(1599, 11)	(308, 6)	(515, 345, 90)

A Dataset and Implementation

A.1 Commonly Used TS Datasets

The information of the experiment datasets used in this paper are summarized as follows: (1) Electricity Transformer Temperature (ETT) dataset Zhou et al. (2021a), which contains the data collected from two electricity transformers in two separated counties in China, including the load and the oil temperature recorded every 15 minutes (ETTh) or 1 hour (ETTh) between July 2016 and July 2018. (2) Electricity (ECL) dataset¹ collects the hourly electricity consumption of 321 clients (each column) from 2012 to 2014. (3) Exchange Lai et al. (2018) records the current exchange of 8 different countries from 1990 to 2016. (4) Traffic dataset² records the occupation rate of freeway system across State of California measured by 861 sensors. (5) Weather dataset³ records every 10 minutes for 21 meteorological indicators in Germany throughout 2020. (6) Solar-Energy Lai et al. (2018) documents the solar power generation of 137 photovoltaic (PV) facilities in the year 2006, with data collected at 10-minute intervals. (7) The PEMS dataset Liu et al. (2022a) comprises publicly available traffic network data from California, collected within 5-minute intervals and encompassing 358 attributes. (8) Illness (ILI) dataset⁴ describes the influenza-like illness patients in the United States between 2002 and 2021, which records the ratio of patients seen with illness and the total number of the patients. The detailed statistics information of the datasets is shown in Table 6, and the dataset information in terms of their size and number of features is summarized in Table 7.

A.2 Implementation Details

The model undergoes training utilizing the ADAM optimizer Kingma and Ba (2015) and minimizing the Mean Squared Error (MSE) loss function. The training process is halted prematurely, typically within 10 epochs. The DistPred architecture solely comprises the embedding layer and backbone architecture, devoid of any additional introduced hyperparameters. During model validation, two evaluation metrics are employed: CRPS, QICE, PICP, MSE and MAE. Given the potential competitive relationship between the two indicators, MSE and MAE, we use the average of the two ($\frac{MSE+MAE}{2}$) to evaluate the overall performance of the model.

¹<https://archive.ics.uci.edu/ml/datasets/ElectricityLoadDiagrams20112014>

²<http://pems.dot.ca.gov>

³<https://www.bgc-jena.mpg.de/wetter>

⁴<https://gis.cdc.gov/grasp/fluview/fluportaldashboard.html>

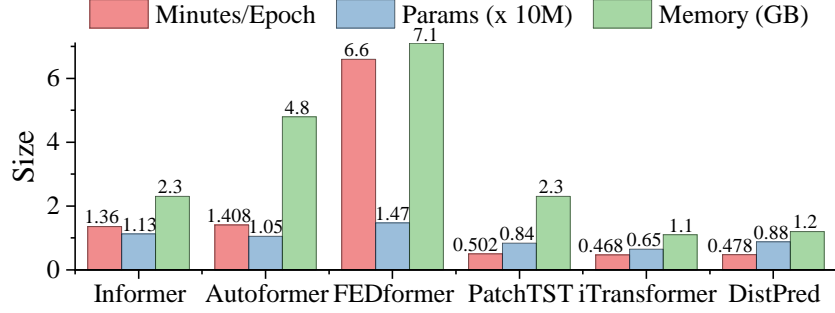


Figure 10: QQ-plots and histograms of response variable.

Table 8: Comparison of DistPred trained with Gaussia distribution.

	Ettm2			Traffic			Exchange			Weather		
	CRPS	MSE	MAE	CRPS	MSE	MAE	CRPS	MSE	MAE	CRPS	MSE	MAE
DistPred	0.189	0.12	0.256	0.161	0.137	0.216	0.343	0.426	0.456	0.023	0.002	0.028
DistPred-G	4391.80	7.61	1.73	2329.05	276.51	6.35	177.92	16.52	1.72	229.58	2.27	0.17

B Comparisons of Model Efficiency in Time Series Forecasting

We evaluate the inference time and size of DistPred (mean only) in comparison to other Transformer-based models, as shown in Fig. 10. It can be observed that DistPred’s runtime, model size, and memory usage do not significantly increase compared to other models.

C Distribution Free v.s. Distribution Related

If we assume that the response variable follows a continuous distribution, as done in (Salinas et al., 2020) where \hat{y} is assumed to be followed Gaussian distribution, we can provide an analytical formula for the Gaussian likelihood. Specifically, if $\hat{y} \sim \mathcal{N}(\mu, \sigma)$, then we can parametrize the Gaussian likelihood using its mean and standard deviation,

$$\mathcal{L}_G(\hat{y}|\mu, \sigma) = (2\pi\sigma^2)^{-\frac{1}{2}} \exp(-(\hat{y} - \mu)^2 / (2\sigma^2)). \quad (16)$$

Then, we can train DistPred utilizing Eq. 16 as the loss function. As shown in Table 8, DistPred exclusively provides the mean and variance of the response variable.

D DistPred for Time Series with Missing Values

The proposed DistPred is equipped to handle time series with missing values scenarios, as both imputation and forecasting are done in a similar manner. Our experiments have demonstrated that DistPred remains SOTA even when a substantial portion of the data is missing. Specifically, in cases where 80% of the PhysioNet2012 data points were absent, the model still maintained competitive performance, as shown in Table 9.

E Univariate Time Series Forecasting

The full results for univariate TS forecasting are presented in Table 10. As other models, e.g., iTransformer Liu et al. (2023) and PatchTST Nie et al. (2022) do not offer performance information for all prediction lengths, we compare our method with those that provide comprehensive performance

Table 9: Comparison of DistPred with other SOTA models when time series with missing values.

Model	M-RNN	GP-VAE	BRITS	USGAN	CSDI	TimesNet	Transformer	SAITS	DistPred
MSE	0.864±0.002	0.433±0.011	0.325±0.002	0.306±0.001	0.260±0.05	0.272±0.006	0.225±0.002	0.218±0.002	0.204±0.002
MAE	0.674±0.001	0.4±0.007	0.246±0.001	0.25±0.001	0.211±0.003	0.266±0.007	0.209±0.002	0.202±0.002	0.196±0.002

Table 10: Univariate time series forecasting results on benchmark datasets.

Model	DistPred-96					FEDformer-96		Autoformer-96		Informer-96		LogTrans-96		Reformer-96		
	Length	CRPS	QICE	PICP	MSE	MAE	MSE	MAE	MSE	MAE	MSE	MAE	MSE	MAE	MSE	MAE
ETTh1	96	0.134	6.341	96.936	0.057	0.182	0.079	0.215	<u>0.071</u>	<u>0.206</u>	0.193	0.377	0.283	0.468	0.532	0.569
	192	0.152	3.766	97.479	0.073	0.207	<u>0.104</u>	<u>0.245</u>	0.114	0.262	0.217	0.395	0.234	0.409	0.568	0.575
	336	0.162	3.762	98.071	0.080	0.221	0.119	0.270	<u>0.107</u>	<u>0.258</u>	0.202	0.381	0.386	0.546	0.635	0.589
	720	0.164	4.176	88.437	0.082	0.226	0.142	0.299	<u>0.126</u>	<u>0.283</u>	0.183	0.355	0.475	0.628	0.762	0.666
	Avg	0.153	4.505	95.235	0.073	0.209	0.111	0.257	<u>0.105</u>	<u>0.252</u>	0.199	0.377	0.345	0.513	0.624	0.600
ETTh2	96	0.203	7.511	81.780	<u>0.129</u>	<u>0.276</u>	0.128	0.271	0.153	0.306	0.213	0.373	0.217	0.379	1.411	0.838
	192	0.240	4.164	80.855	0.176	0.327	<u>0.185</u>	<u>0.33</u>	0.204	0.351	0.227	0.387	0.281	0.429	5.658	1.671
	336	0.281	5.482	87.817	<u>0.234</u>	0.348	0.231	<u>0.378</u>	0.246	0.389	0.242	0.401	0.293	0.437	4.777	1.582
	720	0.274	5.820	89.181	<u>0.219</u>	0.379	0.278	0.42	0.268	0.409	0.291	0.439	0.218	0.387	2.042	1.039
	Avg	0.250	5.744	84.908	0.190	0.341	<u>0.206</u>	<u>0.350</u>	0.218	0.364	0.243	0.400	0.252	0.408	3.472	1.283
ETTm1	96	0.095	6.492	88.992	0.029	0.126	<u>0.033</u>	<u>0.140</u>	0.056	0.183	0.109	0.277	0.049	0.171	0.296	0.355
	192	0.117	4.496	92.619	0.044	0.158	<u>0.058</u>	<u>0.186</u>	0.081	0.216	0.151	0.310	0.157	0.317	0.429	0.474
	336	0.137	5.488	92.264	0.058	0.186	0.084	0.231	<u>0.076</u>	<u>0.218</u>	0.427	0.591	0.289	0.459	0.585	0.583
	720	0.163	3.541	95.713	0.080	0.218	<u>0.102</u>	<u>0.250</u>	0.110	0.267	0.438	0.586	0.430	0.579	0.782	0.73
	Avg	0.128	5.004	92.397	0.053	0.172	<u>0.069</u>	<u>0.202</u>	0.081	0.221	0.281	0.441	0.231	0.382	0.523	0.536
ETTm2	96	0.133	9.595	69.279	<u>0.064</u>	0.180	0.063	<u>0.189</u>	0.065	<u>0.189</u>	0.08	0.217	0.075	0.208	0.077	0.214
	192	0.173	7.392	75.604	0.099	0.233	<u>0.110</u>	<u>0.252</u>	0.118	0.256	0.112	0.259	0.129	0.275	0.138	0.290
	336	0.203	8.833	82.711	0.133	0.277	<u>0.147</u>	<u>0.301</u>	0.154	0.305	0.166	0.314	0.154	0.302	0.160	0.313
	720	0.248	5.720	90.470	0.185	<u>0.333</u>	<u>0.219</u>	<u>0.368</u>	0.182	0.335	0.228	0.380	0.160	0.322	0.168	0.334
	Avg	0.189	7.885	79.516	0.120	0.256	0.135	0.278	<u>0.130</u>	<u>0.271</u>	0.147	0.293	<u>0.130</u>	0.277	0.136	0.288
Traffic	96	0.155	4.245	25.012	0.132	0.209	<u>0.170</u>	<u>0.263</u>	0.246	0.346	0.257	0.353	0.226	0.317	0.313	0.383
	192	0.158	3.596	25.458	0.136	0.213	<u>0.173</u>	<u>0.265</u>	0.266	0.37	0.299	0.376	0.314	0.408	0.386	0.453
	336	0.171	3.458	25.146	0.134	0.213	<u>0.178</u>	<u>0.266</u>	0.263	0.371	0.312	0.387	0.387	0.453	0.423	0.468
	720	0.135	3.434	24.926	0.146	0.228	<u>0.187</u>	<u>0.286</u>	0.269	0.372	0.366	0.436	0.437	0.491	0.378	0.433
	Avg	0.161	3.683	25.136	0.137	0.216	<u>0.177</u>	<u>0.220</u>	0.261	0.365	0.309	0.388	0.341	0.417	0.375	0.434
Electricity	96	0.266	5.619	51.949	0.257	0.366	0.262	0.378	0.341	0.438	<u>0.258</u>	<u>0.367</u>	0.288	0.393	0.275	0.379
	192	0.276	5.018	65.785	0.284	0.376	0.316	0.410	0.345	0.428	<u>0.285</u>	<u>0.388</u>	0.432	0.483	0.304	0.402
	336	0.317	4.947	62.019	0.400	0.439	<u>0.361</u>	<u>0.445</u>	0.406	0.470	0.336	0.423	0.430	0.483	0.37	0.448
	720	0.335	5.191	67.705	0.409	0.460	<u>0.448</u>	<u>0.501</u>	0.565	0.581	0.607	0.599	0.491	0.531	0.46	0.511
	Avg	0.299	5.191	61.865	0.337	0.410	<u>0.347</u>	<u>0.434</u>	0.414	0.479	0.372	0.444	0.410	0.473	0.352	0.435
Weather	96	0.019	10.732	61.824	0.0012	0.024	<u>0.0035</u>	0.046	0.0110	0.081	0.004	<u>0.044</u>	0.0046	0.052	0.012	0.087
	192	0.022	10.463	55.581	0.0013	0.027	0.0054	0.059	0.0075	0.067	<u>0.002</u>	<u>0.040</u>	0.006	0.060	0.0098	0.044
	336	0.023	10.271	59.075	0.0021	0.024	0.008	0.072	0.0063	0.062	<u>0.004</u>	<u>0.049</u>	0.006	0.054	0.013	0.100
	720	0.027	10.515	47.492	0.0023	0.033	0.015	0.091	0.0085	0.070	<u>0.003</u>	<u>0.042</u>	0.007	0.059	0.011	0.083
	Avg	0.023	10.495	55.993	0.0023	0.028	0.008	0.067	0.0083	0.0700	<u>0.0033</u>	<u>0.0438</u>	0.0059	0.0563	0.0115	0.0785
Exchange	96	0.182	6.99	94.678	0.110	0.241	<u>0.131</u>	<u>0.284</u>	0.241	0.387	1.327	0.944	0.237	0.377	0.298	0.444
	192	0.263	10.391	82.484	0.204	0.338	<u>0.277</u>	<u>0.420</u>	0.300	0.369	1.258	0.924	0.738	0.619	0.777	0.719
	336	0.376	10.778	87.861	0.401	0.482	<u>0.426</u>	<u>0.511</u>	0.509	0.524	2.179	1.296	2.018	1.0700	1.833	1.128
	720	0.552	9.526	81.032	0.991	0.763	<u>1.162</u>	<u>0.832</u>	1.260	0.867	1.28	0.953	2.405	1.175	1.203	0.956
	Avg	0.343	9.421	86.514	0.426	0.456	<u>0.499</u>	<u>0.512</u>	0.578	0.537	1.511	1.029	1.350	0.810	1.028	0.812
1 st Count	-	-	-	34	37	<u>3</u>	1	0	0	1	1	2	1	0	0	

analysis, including FEDformer Zhou et al. (2022), Autoformer Wu et al. (2021), Informer Zhou et al. (2021a), LogTrans Li et al. (2019) and Reformer Kitaev et al. (2020). This reaffirms the effectiveness of DistPred.